

ARTICLES

An integrated model of kimberlite ascent and eruption

Lionel Wilson¹ & James W. Head III²

Diatremes are carrot-shaped bodies forming the upper parts of very deep magmatic intrusions of kimberlite rock. These unusual, enigmatic and complex features are famous as the source of diamonds. Here we present a new model of kimberlite ascent and eruption, emphasizing the extremely unsteady nature of this process to resolve many of the seemingly contradictory characteristics of kimberlites and diatremes. Dyke initiation in a deep CO₂-rich source region in the mantle leads to rapid propagation of the dyke tip, below which CO₂ fluid collects, with a zone of magmatic foam beneath. When the tip breaks the surface of the ground, gas release causes a depressurization wave to travel into the magma. This wave implodes the dyke walls, fragments the magma, and creates a 'ringing' fluidization wave. Together, these processes form the diatreme. Catastrophic magma chilling seals the dyke. No precursor to the eruption is felt at the surface and the processes are complete in about an hour.

From a geophysical standpoint, kimberlites are fluid-rich materials, ultramafic in overall composition, that extract xenoliths rapidly and erupt explosively from great depths. The presence of diamonds in some kimberlites indicates a source at pressures of at least 6–8 GPa, the pressure at which diamond is stable relative to graphite at mantle temperatures; this corresponds to depths of ~200–250 km. From a petrologic standpoint, kimberlite is a volatile-rich, very-low-silica igneous rock. Mineral deposit geologists view kimberlite as a porphyritic alkalic peridotite with abundant phenocrysts of olivine and phlogopite. Finally, from a volcanologic standpoint, diatremes are funnel-shaped breccia pipes that extend to as much as 2,500 m in depth, and are thought to form¹ by "hydrovolcanic fragmentation and wall rock collapse ...[and]...may underlie maars and grade at depth into dykes." This range of definitions illustrates the diverse nature and unusual properties of diatremes and kimberlites², and suggests why no single model currently exists that successfully explains their often contradictory characteristics. We summarize these characteristics to provide a basis for developing a comprehensive model for the ascent and eruption of kimberlites and the formation of diatremes and associated features.

Background and characteristics

Early studies of kimberlites³ showed that they occur both as carrot-shaped vertical intrusions (pipes or diatremes) and as tabular dykes known as fissure kimberlites, but their connections were not fully appreciated until the early 1970s when the classic analyses of Dawson⁴ and Hawthorne⁵ established the basic principles of kimberlite magmatism. These authors recognized the existence of hot mobile kimberlite magmas capable of undergoing differentiation, the occurrence of pyroclastic and epiclastic kimberlites, and the gradation with increasing depth of diatremes into non-brecciated hypabyssal kimberlites³. From this time on, kimberlites were recognized as volatile-rich ultrabasic magmas, the evolution and emplacement of which could be described in terms of standard processes of differentiation, intrusion and extrusion. Diatremes thus became only one particular manifestation of a more general magmatic style³. This led to the understanding of the relationships between the major components of a kimberlite magmatic system (Fig. 1), which include crater, diatreme

and hypabyssal facies and three textural genetic groups of rocks, each associated with a particular style of magmatic activity (see, for example, refs 3–6). These components are described below.

Crater facies kimberlites include pyroclastic rocks and epiclastic rocks. Kimberlitic magmas rarely produce lava flows but typically form pyroclastics that, where studied in detail⁷, display several types of deposits. From oldest (lowest) to youngest, these can include basal breccias, poorly stratified coarse pyroclastic deposits (tuffs and tuff breccias) containing fragments of kimberlite, country rock and mantle-derived xenoliths, well-stratified tuffs (alternating layers of coarse lapilli-sized tuffs and laminae of finer ash-sized tuffs) and, finally, epiclastic lacustrine deposits. In many cases, graded beds and depositional features seem to be absent, leading to the interpretation that such tuffs are primarily airfall⁷. Fluvial reworking of tuffs in crater lakes produces epiclastic kimberlites. Volumes of pyroclastic deposits are small and they are typically confined to craters and to thinly bedded tuff-rings; subsequent shallow magmatic intrusions or extrusive lava flows do not typically follow pyroclastic eruptions. Erosion usually follows quickly, but marginal slumping and downfaulting may preserve crater rim facies. These deposits have some similarities to hydrovolcanic tuff rings⁸.

Diatreme facies kimberlites underlie crater facies kimberlites (Fig. 1). They occur in carrot-shaped bodies with circular to elliptical cross-sectional areas that have vertical axes and steeply dipping margins that converge and terminate at depth in a root zone, where the diatreme expands, contracts, or splits up into an irregularly shaped multiphase intrusion of hypabyssal kimberlite³. The commonest rocks in the diatreme facies are tuffistic kimberlite breccias, containing pelletal lapilli, abundant angular to rounded country rock inclusions (mostly a few centimetres down to microscopic), and discrete and fractured grains of olivine, garnet and ilmenite mega- and macrocrysts, set in a fine-grained matrix of microcrystalline diopside and serpentine. The matrix quickly undergoes alteration and replacement by clays and secondary calcite³. Typically, one to three texturally distinctive varieties of tuffistic kimberlite breccias are seen in diatreme zones.

Hypabyssal facies kimberlites (Fig. 1) are rocks formed by the crystallization of volatile-rich kimberlitic magma and exhibit igneous

¹Environmental Science Department, Lancaster University, Lancaster LA1 4YQ, UK. ²Department of Geological Sciences, Brown University, Providence, Rhode Island 02912, USA.

textures and effects of magmatic differentiation; often they contain sufficient country rock xenoliths to be called kimberlitic breccias. These occur as dykes and form the root zones of diatremes (Fig. 1). Kimberlitic dykes are typically vertically dipping with 1–3 m widths, but can be up to 10 m wide³, and commonly form swarms of parallel features. Most dykes are single intrusions and pinch out towards the surface, thickening with depth; many show evidence of flow differentiation, glassy selvages are absent, and contact metamorphic effects are slight. Some dykes are observed to expand along strike into lenticular features 10–20 times the dyke width and up to 100 m in length; these are termed ‘blows’ and may represent the lowermost portions of root zone intrusions³. Internal dykes are common in most diatremes and root zones, but are small, rootless, sinuous and pinch out laterally and vertically, cross-cutting intrusions within the pipes but not extending into the surrounding country rock. Most have no preferred orientation and may be localized at the dyke–wall-rock contact or at the contact between discrete intra-diatreme intrusions³. Subsequent or cross-cutting dykes are extremely rare, suggesting that the diatreme-forming event is the closing stage of kimberlitic magmatism. Kimberlitic sills are relatively rare and plutonic kimberlitic complexes are unknown³.

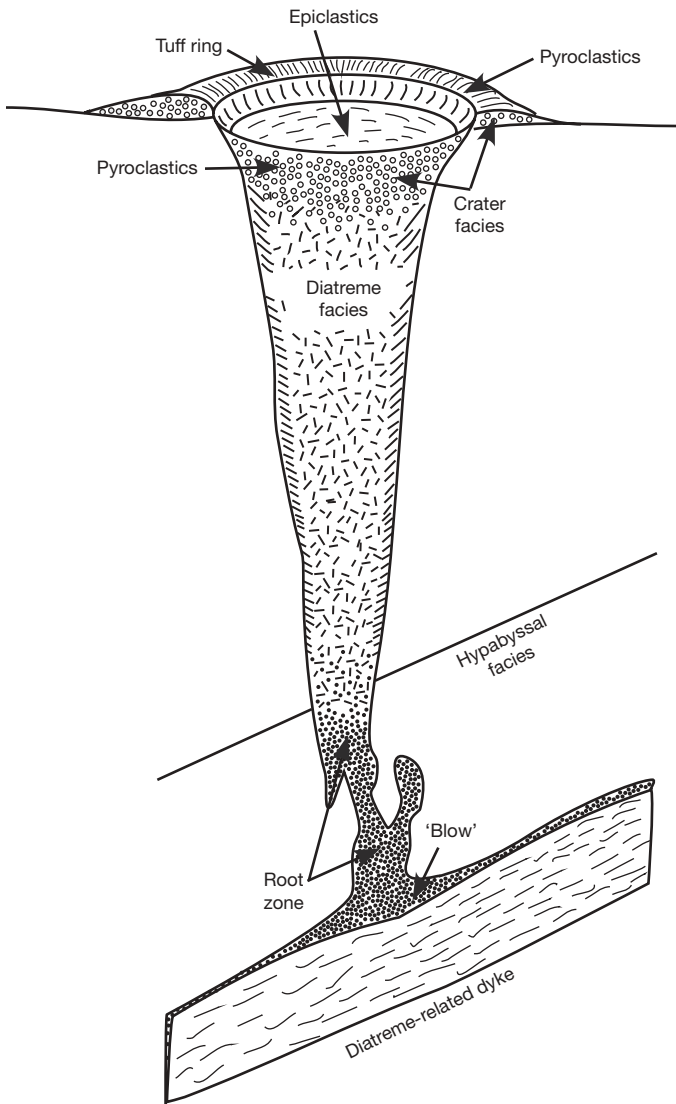


Figure 1 | Model of an idealized kimberlite magmatic system illustrating the relationships between crater, diatreme, and hypabyssal zones and facies rocks. Not to scale. Modified from Fig. 3.1 on page 30 of ref. 3, with kind permission of Springer Science and Business Media.

Summary of distinctive characteristics

The major characteristics that need to be explained in any model for the formation of kimberlite diatremes are summarized in Table 1. Relative to normal magmatic eruptions, the most unusual of these characteristics raise the questions of how is it possible to: (1) transport diamonds from the mantle (where they are stable) to the surface (where they are metastable) fast enough to avoid significant alteration over the intervening range of depths at which they are unstable; (2) transport significant quantities of mantle xenoliths to near-surface levels; (3) produce intrusive pyroclastic kimberlitic material at depths where pressures would normally preclude magma fragmentation by volatile expansion, and then separate most of the volatiles from the pyroclastic materials; (4) generate extensive fracturing and brecciation of host rocks in many parts of the system, with minimal contact metamorphic effects; and (5) produce complex shallow structures (diatremes and root zones) in which an unusual widening of the conduit system occurs, sometimes with extensions that do not connect to the surface, and where complex mixtures of fragmented material and coherent dyke segments are present.

Models for kimberlite emplacement and diatreme

Attempts to explain the characteristics outlined above have included explosive liberation of highly compressed magmatic gases at shallow depths to produce a volcanic vent (diatreme)⁹ and small, subsurface, discrete and repeated upwardly migrating explosions causing explosive boring¹⁰. Fluidization—the transportation and circulation of particles by high-velocity gas flow¹¹—has been extensively applied to the formation of diatremes, with some^{4,12–15} postulating that a gas-charged kimberlite magma breaks through to the surface, and that adiabatic expansion of magmatic gas then enlarges the explosion vent, which is subsequently filled with fluidized fragmented kimberlite that drills upward with a sandblasting effect. On the basis of the similarities of maars/tuff cones to the surface expressions of diatremes, several authors have strongly advocated that diatremes are caused by hydrovolcanic activity, the interaction of magma and near-surface water (for example, refs 16–18): magma rising in pre-existing cracks encounters water-rich zones and produces hydrovolcanic explosions that fragment and chill magma while simultaneously brecciating the country rock. Continued and repetitive activity results in a diatreme, the conduit surrounded by brecciated and spalled rock.

Table 1 | Key characteristics of type 1 kimberlite diatremes

Structure and shape
Distinctive carrot shape of diatreme Three distinctive regions and facies (crater, diatreme and hypabyssal)
Characteristics
Kimberlitic mantle-derived composition and mineralogy Volatile-rich nature of kimberlite magma, dominated by CO ₂ Angular clasts of shallow country rock, typically devoid of kimberlitic coating Pronounced sphericity of lapilli (mostly 1–10 mm in size) Glassy or microcrystalline spherules, implying rapid quenching Smaller amounts of more rounded lower crustal and mantle material, exposed deeper within the diatreme Olivine-cored pelletal lapilli surrounded by usually altered quenched kimberlitic melt or glass
Features usually lacking
Extensive extrusive deposits Thermal metamorphism Exposed plutonic complexes Subsequent dykes Vesicles and composite lapilli
Implications for emplacement models
Apparent rapid emplacement, preventing destruction of diamonds in transit Implied low temperatures of emplacement, despite magmatic transport

The difficulty of having one single mechanism account for the diversity of characteristics of kimberlites and diatremes led Clement^{19,20} to propose more complex models combining different processes (embryonic pipes modified into diatremes by fluidization and fluctuation in magma flow rates, producing changes in pressure and implosion and shattering of country rocks). Mitchell³ suggested that no single process could be responsible for the formation of the complex structure of kimberlites and diatremes and that root zone processes may combine with hydrovolcanic processes at shallower depths to produce the observed features³. Using new insights from the fluid mechanics of dyke propagation, we propose a model that accounts for most of the features summarized in Table 1.

A new model for ascent and eruption

We propose that essentially all of the rise of kimberlitic magma to the surface takes place via rapid propagation of a dyke from unusually great depths (Fig. 2) rather than the much slower propagation of a diapir to shallower depths before transitioning to a dyke. This very deep dyke initiation and propagation minimizes thermodynamic problems associated with transporting diamonds from mantle depths to the surface. Dyke propagation is initiated in a diapirically rising^{21,22} CO₂-rich mantle source region^{23,24} when the percentage of partial melt in the source exceeds the critical level allowing upward drainage to begin at a rate so large that the maximum strain rate at which the matrix can deform plastically is exceeded^{25,26}. Previous kimberlite dyke propagation analyses have emphasized magma flow once a dyke has reached the surface. Our new model focuses on the pressure distribution in a dyke during its ascent.

Stage 1. This stage involves dyke tip propagation out of a deep source region and CO₂ fluid segregation. The dyke sets out from the mantle source^{27,28} at a depth of ~250 km, where the pressure is ~8 GPa (Fig. 2a). The magma in the dyke could contain as much as 20 wt% of CO₂ (ref. 29), and the pressure-dependent solubility of this volatile is such that the dyke tip pressure, in attempting to reach the lowest possible value in order to maximize the magma flow speed, would initially be buffered at ~2 GPa by the release of 90% of the available CO₂ (ref. 25) as a supercritical fluid filling the cavity behind the dyke tip. The difficulty of diffusing the volatile phase into the cavity causes a foam layer to rapidly develop beneath the tip cavity (Fig. 2b). Fluid bubbles in the foam burst into the cavity, and the cavity pressure decreases³⁰ to the value at which the bubble volume fraction is ~0.7–0.8, the condition under which³¹ volcanic foams commonly disintegrate into a continuous volatile phase containing entrained droplets of the magmatic liquid. The CO₂ density at which ~20 wt% forms bubbles occupying ~75% of the volume at magmatic temperatures is ~220 kg m⁻³. Using thermodynamic data for supercritical CO₂, this corresponds to a pressure of ~70 MPa. Thus, the pressure decreases upward from ~2 GPa to ~70 MPa across the foam layer. The supply of CO₂ is constantly renewed by streaming of degassed magma to the sides of the dyke as the dyke grows both upward and laterally, exposing fresh undegassed magma in the dyke centre. The tip cavity grows in length in a manner controlled by the elastic stresses acting over the upper part of the dyke³² and may be 2–4 km long by the time the dyke tip is near the surface.

Stage 2. This stage involves dyke ascent and wall fracturing. As magma ascends from the source region at a pressure of ~8 GPa to the base of the foam layer at ~2 GPa it will cool adiabatically from ~1,650 K to ~1,450 K (ref. 33). Its passage through the foam layer from a pressure of ~2 GPa to ~70 MPa can be treated as the adiabatic expansion of a pseudo-gas³⁴, resulting in cooling from ~1,450 K to ~1,110 K. The pressure difference in excess of the static weight of the magma column (source pressure minus tip pressure) will be fixed at ~8 GPa, and on subtracting the static weight of the magma column the pressure difference driving the magma motion is found to vary from ~8 GPa at great depth to ~1 GPa near the surface. Dividing by the length of the magma column yields a pressure gradient ranging from ~1 MPa m⁻¹ at great depth to ~4 kPa m⁻¹ near the surface. The average pressure

gradient of more than 60 kPa m⁻¹ is ~20 times larger than the gradients driving basaltic eruptions from shallow magma reservoirs³⁵ and leads to the magma flowing upward in a turbulent manner with an average rise speed of ~30–50 m s⁻¹, implying an extremely short transit time of only about 1 hour (ref. 36; Fig. 2c).

The dyke tip pressure is buffered at ~70 MPa during the entire rise to the surface but the external pressure decreases owing to the decreasing overburden. Over most of the rise distance of the dyke, wall rocks adjacent to the propagating dyke tip region are fractured in tension (Fig. 2c). Country rock is torn from the walls to become xenoliths, and quickly sinks through the CO₂ fluid to become engulfed by and incorporated into the underlying magmatic foam. Over the last several kilometres of magma rise, the stress across the dyke walls changes from tensile to compressive, with the possibility of intrusion of small dykelets owing to the decreasing overburden pressure. The relative abundance of xenoliths produced by wall rock fracturing will be a function of rock strength and position in the crust relative to the evolving differential stress; the most important factor will be the elapsed time over which the wall rocks are exposed to dyke emplacement, favouring deep xenoliths.

Stage 3. Next, the dyke tip breaks the surface, vents CO₂ gas and implodes the walls. The propagating dyke is convex upward along its length and first reaches the surface at its highest central point, immediately starting to vent the CO₂ fluid from the dyke tip cavity (Fig. 2d). On being exposed to the surface, the supercritical fluid expands adiabatically to atmospheric pressure to become a subcritical gas, producing an initial vulcanian explosion. Its upward velocity increases from the ~20 m s⁻¹ rise speed of the dyke to a speed that depends on the amount of clastic material which it carries. If a pure gas is released its speed will be ~1.4 km s⁻¹ and it will have cooled adiabatically to ~300 K. If the gas is loaded with all of the magma in the form of small droplets its speed will be ~600 m s⁻¹ and its temperature ~680 K, and if it is loaded by magma droplets and an equal mass of host rock wall fragments, then the values will be ~300 m s⁻¹ and ~500 K.

The expansion wave causing this violent acceleration of the cavity fluid will propagate downward through it at about half the speed of sound in CO₂ at the magmatic temperature (that is, ~300 m s⁻¹) emptying a typically 3-km-deep cavity in ~10 s. The mixture of gas and entrained particles ejected into the atmosphere will produce a classic Prandtl jet that will begin to interact with the surrounding air to produce a plinian or sub-plinian eruption plume (Fig. 2e). The dyke will rapidly centralize along the widest portion (almost certainly the central part that reaches the surface first and within which the rise speed of magma and gas is greatest) and the remainder of the upper part of the gas-filled dyke will rapidly close. This produces a linear fractured and crushed zone with little to no evidence of associated magma, in the centre of which is a much less elongate central vent. Within this vent, the break-through and the ensuing gas jet will rip wall rock from the uppermost country rock, and the proportion of shallow country rock should be high in the initial ejecta deposits around the vent. Simultaneously, the sharp decrease in pressure caused by the gas venting will fracture and implode the walls of the upper part of the dyke.

Stage 4. The depressurization wave initiated by the gas venting next propagates down through the layer of magmatic foam at about half the speed of sound in the foam (that is, ~50 m s⁻¹; ref. 37), expanding the bubbles and disrupting the foam into magma droplets and released gas (Fig. 2f). The wave continues into the underlying magma at about half the speed of sound in the bubble-free liquid (that is, ~800 m s⁻¹), and more CO₂ is released in the magma-filled portion of the dyke, forming additional foam which also expands and is disrupted (Fig. 2f). In both cases the assemblage of gas and entrained magma droplets will cool from ~1,110 K to ~680 K as long as the front of the expansion wave is maintained at atmospheric pressure. During the disruption and expansion process (Fig. 2f), surface tension will form the resulting liquid fragments into spheres to optimize the surface area to volume ratio. These spheres would incorporate any solid particles in the rising magma (olivine

phenocrysts, xenolithic grains) that had acted as nuclei for the volatile bubbles, and the very rapid adiabatic cooling of these particles would produce glassy or microcrystalline spherules, cored by phenocrysts and xenoliths, the pellet lapilli of the tuffisitic kimberlite breccias. Cooling would be so rapid (going from magmatic to room temperature in seconds) that welding of particles and agglutination would be minimized.

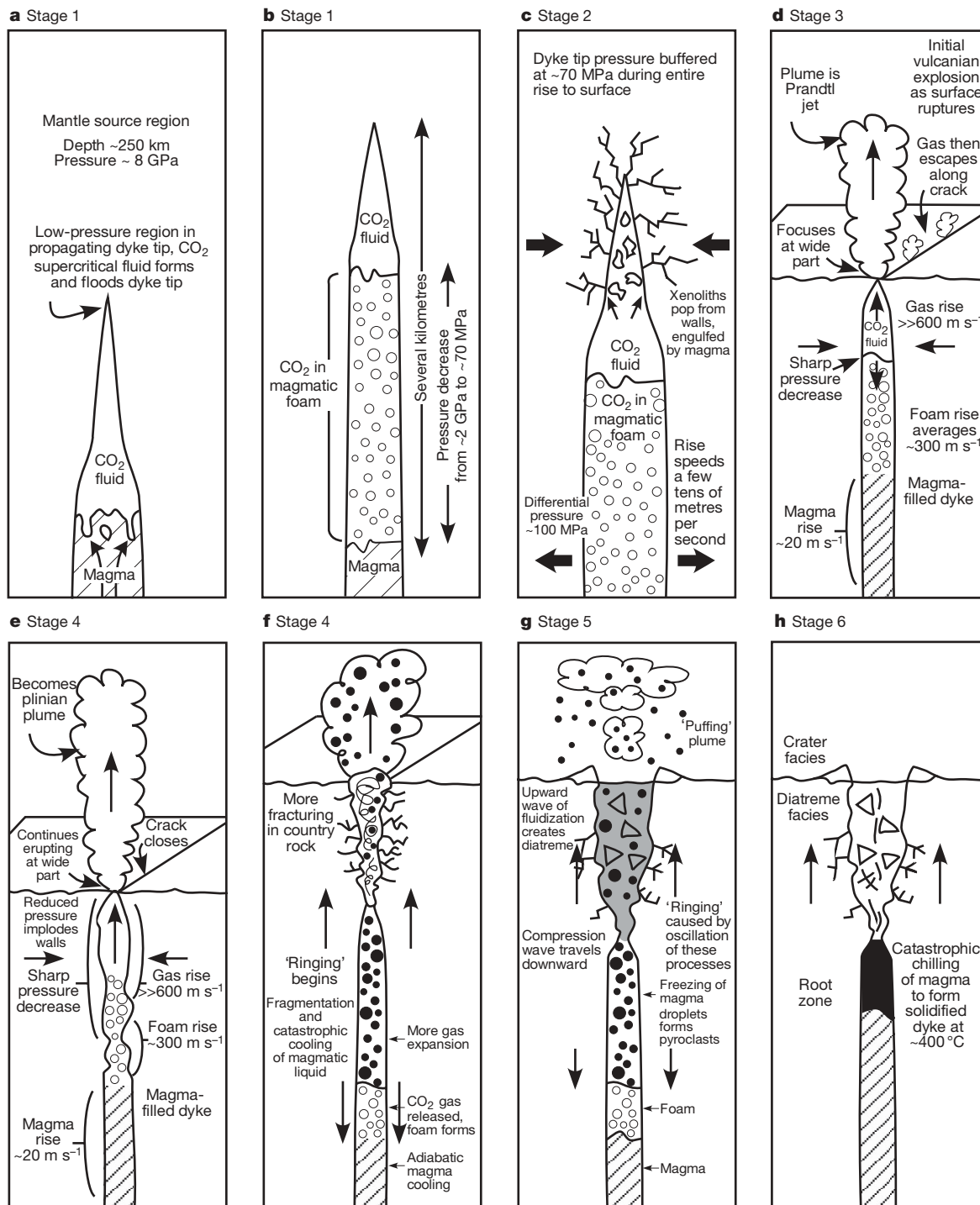


Figure 2 | Sequence of events in the generation, ascent and eruption of kimberlitic magmas and diatreme formation (see text for details).

a, b, Stage 1 involves dyke tip propagation out of a deep source region and CO₂ fluid segregation (**a**). As the dyke tip propagates, disequilibrium produces CO₂/magmatic foam (**b**). **c,** Stage 2 involves dyke ascent and wall fracturing. **d,** In stage 3, the dyke tip breaks the surface, vents CO₂ gas and implodes the walls. **e, f,** In stage 4, gas venting causes a depressurization wave

Stage 5. In this stage, gas expansion creates an upward fluidization wave and accelerates chilled pyroclasts. The gas expansion in the dyke caused by the gas venting accelerates the gas into the shattered country rock and produces an upward wave of fluidization that is the major cause of the formation of the diatreme structure (Fig. 2g). The combination of foam disintegration in the upper part of the dyke below the continuous gas phase, and the further foam formation and

to propagate into the magmatic foam (**e**) and the underlying magma and country rock (**f**); the diatreme begins to form. **g,** In stage 5, gas expansion creates an upward fluidization wave and accelerates chilled pyroclasts. The vent clogging reduces the pyroclastic escape route, increasing the pressure, which causes 'ringing'. **h,** Stage 6 is the aftermath of the event. The dyke solidifies and the deflated, completed diatreme will be porous and cone-shaped, surrounded by a crater rim of breccia and pyroclastic deposits.

disintegration in the magma below the initial magmatic foam zone, is responsible for the upward fluidization wave. This produces a cold stream of gas through the upper part of the zone, which contains cooled spherules and fine-grained magmatic particles that migrate through the upper fractured zone and vent to the surface (Fig. 2f). Very quickly, however, partial clogging of the pathways and increasing path length cause a growing pressure gradient to be developed in the upper part of the system, and the information that this is occurring propagates downward as a wave of compression (Fig. 2g).

Variations in pressure will cause instabilities in the gas exsolution process and gas flow speed and this will introduce cyclic waves of gas release, pressure changes and venting. A series of fluidization waves (a 'ringing') will propagate through the system. Given the low speed of sound in the complex gas/clast/bubbly liquid mixture, this may last for several tens of minutes. During this time, continual readjustments in the diatreme will be taking place as compression and decompression waves propagate back and forth, and a flow of cool gas transporting particles will permeate the diatreme zone and vent to the surface. This fluidization will cause sorting in the brecciated diatreme zone and will allow settling of large blocks of the country rock from the upper part of the column down into deeper parts of the diatreme. The disruption phase will also serve to modify, distort and destroy evidence of earlier stages of dyke emplacement. During this time, the magma deeper in the dyke itself will quickly undergo catastrophic adiabatic chilling (Fig. 2h) and thus will cease to rise into the diatreme. The deposits on the surface should be characterized by a basal coarse breccia from the initial venting, followed by coarse fragments, xenoliths and lapilli from the initial magmatic foam phase, followed by deposits dominated by products from the second magmatic foam phase (chilled lapilli and ash). The extreme cooling of the magma will inhibit its rise into the vent and any subsequent eruption of surface flows. Diamonds are emplaced into the diatreme facies as part of the kimberlite magma from below the gas and foam zones, where the melt stays at high pressure.

Stage 6. In the aftermath of the event, the deposits will be characterized by a porous, cone-shaped diatreme surrounded by a crater rim of breccia and pyroclastic deposits (Fig. 1). If the diatreme forms in an active groundwater area, a crater lake is likely to form and groundwater will permeate the diatreme, quickly altering the primary mineralogy. Although the predicted surface deposits are similar in some ways to those of tuff cones and maars formed by hydrovolcanic processes, no part of this model requires interaction of the rising dyke with groundwater. Such an interaction could happen, but the very rapid chilling of the magmatic foams minimizes the likelihood of prolonged and repetitive hydrovolcanic eruptions occurring during the formation of diatremes.

Conclusions

This model for the ascent and eruption of CO₂-rich kimberlitic magma (Fig. 2) accounts for the major observational characteristics of kimberlites associated with diatremes^{1,3}, summarized in Fig. 1 and Table 1. The termination of the eruption immediately after diatreme formation, probably within at most a few tens of minutes of the onset of eruption, is a direct consequence of the extreme cooling of magma during the large pressure reductions that occur on venting to the atmosphere. The subsequent very rapid pressure and temperature fluctuations lead to the formation of a diverse suite of rock types in the intrusive deposits that characterize these eruptions. Only limited amounts of pyroclastic materials are expected to be erupted onto the surface. Cases in which abundant CO₂ was lacking in deep melt sources and water was the dominant mantle volatile could result in kimberlite dyke intrusions and eruptions without diatreme formation. Some such events could be of a more protracted nature, building up extensive surface deposits similar to those of traditional basaltic pyroclastic eruptions^{1,15}.

Received 1 November 2006; accepted 19 February 2007.

1. Vespermann, D. & Schmincke, H. in *Encyclopedia of Volcanoes* (ed. Sigurdsson, H.) 683–694 (Academic Press, San Diego, California, 2000).

2. Field, M. & Scott Smith, B. in *Proc. 7th Int. Kimberlite Conf.* (eds Gurney, J. J., Gurney, J. L., Pascoe, M. D. & Richardson, S. H.) Vol. 1, 214–237 (Red Roof Design, Cape Town, 1999).
3. Mitchell, R. H. *Kimberlites* (Plenum, New York, 1986).
4. Dawson, J. Advances in kimberlite geology. *Earth Sci. Rev.* **7**, 187–214 (1971).
5. Hawthorne, J. Model of a kimberlite pipe. *Phys. Chem. Earth* **9**, 1–15 (1975).
6. Clement, C. R. & Reid, A. M. in *Fourth Int. Conf. on Kimberlites and Related Rocks* Vol. 14, 632–646 (Geological Society of Australia, Perth, 1989).
7. Mannard, G. The surface expression of kimberlite pipes. *Proc. Geol. Assoc. Canada* **19**, 15–21 (1968).
8. Wohletz, K. & Sheridan, M. Hydrovolcanic explosions: II, Evolution of basalts tuff rings and tuff cones. *Am. J. Sci.* **283**, 385–413 (1983).
9. Wagner, P. A. *The Diamond Fields of Southern Africa* 1–355 (The Transvaal Leader, Johannesburg, 1914).
10. Kostrovitsky, S. I. *Physical Conditions, Hydraulics and Kinematics of Emplacement of Kimberlite Pipes* 1–95 (Nauka, Novosibirsk, 1976).
11. Reynolds, D. L. Fluidization as a geological process and its bearing on the problem of intrusive granites. *Am. J. Sci.* **255**, 577–613 (1954).
12. McGetchin, T. R. & Ulrich, G. W. Xenoliths in maars and diatremes with inferences for the Moon, Mars, and Venus. *J. Geophys. Res.* **78**, 1833–1853 (1973).
13. McGetchin, T. R., Nikharj, Y. S. & Chodas, A. A. Carbonatite-kimberlite relations in the Cane Valley diatreme, San Juan County, Utah. *J. Geophys. Res.* **78**, 1854–1869 (1973).
14. Wyllie, P. J. The origin of kimberlite. *J. Geophys. Res.* **85**, 6902–6910 (1980).
15. Skinner, E. & Marsh, J. Distinct kimberlite pipe classes with contrasting eruption processes. *Lithos* **76**, 183–200 (2004).
16. Lorenz, V. in *Physics and Chemistry of the Earth* Vol. 9, 17–27 (Pergamon Press, Oxford, 1975).
17. Lorenz, V., Zimanowski, B., Buttner, R. & Kurszlaukis, S. in *Proc. VII Int. Kimberlite Conf.* (eds Gurney, J. J., Gurney, J. L., Pascoe, M. D. & Richardson, S. H.) Vol. 2, 522–528 (Red Roof Design, Cape Town, 1999).
18. Wolfe, J. A. Fluidization versus phreatomagmatic explosions in breccia pipes. *Econ. Geol.* **75**, 1105–1111 (1980).
19. Clement, C. R. The origin and infilling of kimberlite pipes. In *Extended Abstracts, Kimberlite Symposium II*, Cambridge (Geology Dept, DeBeers Consolidated Mines Ltd, 1979).
20. Clement, C. R. A Comparative Geological Study of Some Major Kimberlite Pipes in the Northern Cape and Orange Free State. PhD thesis, Univ. Cape Town (1982).
21. Green, H. W. & Gueguen, Y. Origin of kimberlite pipes by diapiric upwelling in the upper mantle. *Nature* **249**, 617–620 (1974).
22. Kramers, J. D., Smith, C. B., Lock, N. P., Harmon, R. S., Boyd, F. R. Can kimberlites be generated from an ordinary mantle? *Nature* **291**, 53–56 (1981).
23. Wyllie, P. in *Proc. 2nd Int. Kimberlite Conf.* (eds Meyer, H. and Boyd, F. R.) Vol. 1, 319–329 (AGU, Washington DC, 1979).
24. Wyllie, P. & Ryabchikov, I. D. Volatile components, magmas, and critical fluids in upwelling mantle. *J. Petrol.* **41**, 1195–1206 (2000).
25. Anderson, O. L. in *Proc. 2nd Int. Kimberlite Conf.* (eds Meyer, H. and Boyd, F. R.) Vol. 1, 344–353 (AGU, Washington DC, 1979).
26. Sleep, N. H. Tapping of melt by veins and dikes. *J. Geophys. Res.* **93**, 10255–10272 (1988).
27. Lister, J. R. Buoyancy-driven fluid fracture: The effects of material toughness and of low-viscosity precursors. *J. Fluid Mech.* **210**, 263–280 (1990).
28. Rubin, A. M. Dikes vs. diapirs in viscoelastic rock. *Earth Planet. Sci. Lett.* **119**, 641–659 (1993).
29. Wyllie, P. J. & Huang, W. L. Influence of mantle CO₂ in the generation of carbonatites and kimberlites. *Nature* **257**, 297–299 (1975).
30. Wilson, L. & Head, J. W. Deep generation of magmatic gas on the Moon and implications for pyroclastic eruptions. *Geophys. Res. Lett.* **30**, doi:10.1029/2002GL016082 (2003).
31. Wilson, L., Sparks, R. S. J. & Walker, G. P. L. Explosive volcanic eruptions—IV. The control of magma chamber and conduit geometry on eruption column behavior. *Geophys. J. R. Astron. Soc.* **63**, 117–148 (1980).
32. Lister, J. R. Buoyancy-driven fluid fracture: Similarity solutions for the horizontal and vertical propagation of fluid-filled cracks. *J. Fluid Mech.* **217**, 213–239 (1990).
33. Hess, P. *Origins of Igneous Rocks* 1–336 (Harvard Univ. Press, Cambridge, Massachusetts, 1989).
34. Kieffer, S. W. Blast dynamics at Mount St. Helens on 18 May 1980. *Nature* **291**, 568–570 (1981).
35. Wilson, L. & Head, J. W. Ascent and eruption of basaltic magma on the Earth and Moon. *J. Geophys. Res.* **86**, 2971–3001 (1981).
36. Canil, D. & Fedortchouk, Y. Garnet dissolution and the emplacement of kimberlites. *Earth Planet. Sci. Lett.* **167**, 227–237 (1999).
37. Kieffer, S. W. Sound speed in liquid-gas mixtures: Water-air and water-steam. *J. Geophys. Res.* **82**, 2895–2904 (1977).

Supplementary Information is linked to the online version of the paper at www.nature.com/nature.

Acknowledgements This work was supported in part by a grant from the National Aeronautics and Space Administration to J.W.H.

Author Information Reprints and permissions information is available at www.nature.com/reprints. The authors declare no competing financial interests. Correspondence and requests for materials should be addressed to J.W.H. (james_head@brown.edu).